Atmospheric Environment Vol. 27A, No. 17/18, pp. 2927–2934, 1993.
Printed in Great Britain.

0004–6981/93 $6.00 + 0.00

SULFUR DIOXIDE REACTIONS ON ICE SURFACES: IMPLICATIONS FOR DRY DEPOSITION TO SNOW

MARTHA H. CONKLIN,* RICHARD A. SOMMERFELD,† S. KAY LAIRD† and JOHN E. VILLINSKI*

*Department of Hydrology and Water Resources, The University of Arizona, Tucson, AZ 85721, U.S.A. and †Rocky Mountain Experiment Station, U.S.D.A. Forest Service, 240 West Prospect Street, Fort Collins, CO 80526, U.S.A.

(*First received* 3 *April* 1992 *and in final form* 7 *September* 1992)

Abstract—Controlled exposure of ice to a reactive gas, SO_2, demonstrated the importance of the chemical composition of the ice surface on the accumulation of acidity in snow. In a series of bench-scale continuous-flow column experiments run at four temperatures (−1, −8, −30 and −60°C), SO_2 was shown to dissolve and to react with other species in the ice–air interfacial region at temperatures approaching the melting point of ice. Experiments consisted of passing air containing SO_2 through glass columns packed with 100-μm ice spheres of varying bulk composition (0–5 μM H_2O_2, and 0–1 mM NaCl), and analysing SO_2 in the air and SO_4^{2-} in the ice. At all temperatures (−60 to −1°C), increased retention volumes were found for increasing ionic strength and oxidant concentration. At the coldest temperatures and with no NaCl, increased retention volumes for −60 vs −30°C are consistent with SO_2 uptake by physical adsorption. At warmer temperatures, −8 and −1°C, the observed tailing in the sorption curves indicated that other processes besides physical adsorption were occurring. The desorption curves showed a rapid decrease for the warmer temperatures, indicating the sorbed SO_2 is irreversibly oxidized to SO_4^{2-}. Results indicate that aqueous-phase reactions can occur below −8°C (i.e. −30 and −60°C). Results for different salt concentrations show that increasing ionic strength facilitates SO_2 oxidation at colder temperatures, which is consistent with freezing point depression. One environmental implication is that snowpacks in areas with background SO_2, can accumulate acidity during the winter months. As acidity accumulates, the solubility of SO_2 will decrease causing a concomitant decrease in the air-to-surface flux of SO_2. Modeling dry deposition of gases to snow surfaces should incorporate the changing composition of the ice surface.

Key word index: Sulfur dioxide, dry deposition, ice, snow, hydrogen peroxide, ice–air interface, pre-melt layer, laboratory study.

INTRODUCTION

Dry deposition is part of the overall atmosphere–surface exchange process and is the result of a net balance between the atmosphere-to-surface fluxes and the surface-to-atmosphere fluxes. The process of dry deposition is usually separated into three steps corresponding to: (1) atmospheric transport to a quasi-laminar sublayer above the surface, (2) transport through the quasi-laminar sublayer and (3) deposition to the surface. A resistance is associated with each step and the flux is determined by a concentration difference across the resistances in series. The importance of the third resistance, surface interactions, is highly dependent on the substance being deposited and the condition of the surface. For SO_2, it appears that the surface resistance may be controlled by reactions on the surfaces of the ice crystals that comprise the snow. Experiments by Valdez *et al.* (1987) on the uptake of SO_2 on natural snow found evidence that the sorbed SO_2 oxidized readily. They tentatively identified the oxidant as H_2O_2, as measurable amounts of H_2O_2 have been found in snowpacks worldwide (e.g. Neftel *et al.*, 1984; Gunz and Hoffmann, 1990).

The rates of uptake of reactive gases on ice surfaces depend on the chemical composition (i.e. concentrations of oxidant and ionic strength) and the physical characteristics (liquid-like characteristics and surface area) of the surface layer. Studies on non-reactive gases (NO and SO_2 in systems without oxidants) suggest that two processes are involved in the sorption of gases to ice surfaces (Sommerfeld and Lamb, 1986; Clapsaddle and Lamb, 1989; Sommerfeld *et al.*, 1992). At temperatures below −10°C, the amount of uptake increases with decreasing temperature. This is consistent with physical adsorption of gases on an ice surface. At temperatures above −10°C, the uptake of NO (a sparingly soluble gas) was shown to exhibit a temperature dependence that suggested a surface pre-melt layer had started to form (Sommerfeld *et al.* 1992).

In this work, the amount of uptake of SO_2 was studied as a function of salt content, oxidant concentration and temperature of the ice. By studying a gas with understood reaction mechanisms in aqueous systems (e.g. Hoffmann and Calvert, 1985) over a wide range of temperatures, we hypothesized that we would be able to determine under what conditions aqueous-

phase reactions occurred on the ice surfaces. Data will assist in modeling dry deposition of gases to snowpacks and air–snow exchange in general.

METHODS

Ice spheres of 100-μm radius were produced using the technique of Sommerfeld and Freeman (1988). Briefly, five different solutions containing combinations of oxidant ($H_2O_2 = 0$ and 5 μM) and salt (NaCl = 0, 10 and 1000 μM), were made using deionized water from a Barnstead Nanopure water-purification unit. NaCl was from Fisher Scientific, ACS certified, and contained 0.4 ppm Fe. H_2O_2 (30%) was a Mallinckrodt Analytical Reagent. The solution, flowing at rates of 30–50 cm^3 min^{-1}, was directed through a syringe to the tip of a sonic nebulizer. A frequency of 20 kHz was chosen to produce 100-μm ice spheres because Perla's (1978) calculations indicated that significant changes of the specific surface area of ice spheres of this radius of curvature take on the order of months. This was important, as surface area was assumed to remain constant for the time span of the experiments (hours). After the droplets were formed, they fell into a dewar flask filled with liquid N_2, to ensure quick freezing. To reduce risk of contamination (and noise) there was a plastic shield around the horn and the dewar. To check for contamination, some of the ice from each batch was analysed on the ion chromatograph; concentrations of SO_4^{2-} were measured to be 18 ± 6 ppb in the blanks. The blank concentrations were subtracted from our results. It was assumed that no H_2O_2 was lost during the freezing process; this has been confirmed by a study by Iribarne and Pyshnov (1990). There was a 200-μm sieve below the surface of the liquid N_2 to remove any coarser particles formed when stray water drops fell in the flask. The frozen ice spheres were packed into glass columns (12.5 cm length, 2.5 cm dia.) that had the inside pre-coated with ice, and were subsequently sintered at -25°C for at least 3 days to remove regions of high negative curvature. The average surface area was 17 ± 6 mm^2 mm^{-3}. Pore volumes (i.e. volume of void space inside the column) were measured gravimetrically and average values are 24.8 ± 0.9 cm^3; $\pm$ indicates 95% confidence intervals.

During the experiment, the ice columns were placed into a constant-temperature oven (Despatch model 926D) and exposed to a constant concentration of SO_2. Four temperatures were studied: -1, -8, -30 and -60°C. The experimental apparatus is similar to that used by Sommerfeld and Lamb (1986; see Fig. 1). Two gas streams SO_2 and Air Products artificial air, were mixed upstream of the column to achieve SO_2 concentrations of 89 or 69 ppbv (due to using two different cylinders of SO_2); mass flow controllers (Matheson) were used to control the flow and achieve 600 sccm (as required by the detector). This resulted in typical column residence times of 2.5 s; experiments lasted up to 6 h. To ensure no sublimation or deposition of the ice, the air was saturated at the appropriate temperature before mixing with SO_2 (the SO_2 flow rate was approximately two orders of magnitude smaller than the air flow rate). The valves on the apparatus were computer controlled and data were collected using the program ASYST. The outflow of SO_2 was constantly monitored using a pulsed ultraviolet sulfur analyser (TECO 43). The sorption limbs of the breakthrough curves were obtained by saturating the column with SO_2 (saturation was defined as when the output concentration equaled the input concentration, C_o). Then SO_2 was desorbed by passing SO_2-free air through the column; this portion of the breakthrough curve is referred to as the desorption limb. To smooth the data, an average was taken of every five data points, with the center data point weighted by a factor of two. Any instrument bias was then removed, as there was considerable drift of the SO_2 analyser (due to the aging condition of the detector), and the data normalized by the input concentration (C_o). It should be noted that the drift made it difficult to identify when C_o was achieved. We estimate the error could be in the range of 10%. This could result in significant errors in calculating the total amount of SO_2 sorbed from these curves. Good qualitative reproducibility, however, was achieved with the breakthrough curves. Quantitative data from the breakthrough curves were less reliable because of instability of the SO_2 detector, so we did not report retention volumes.

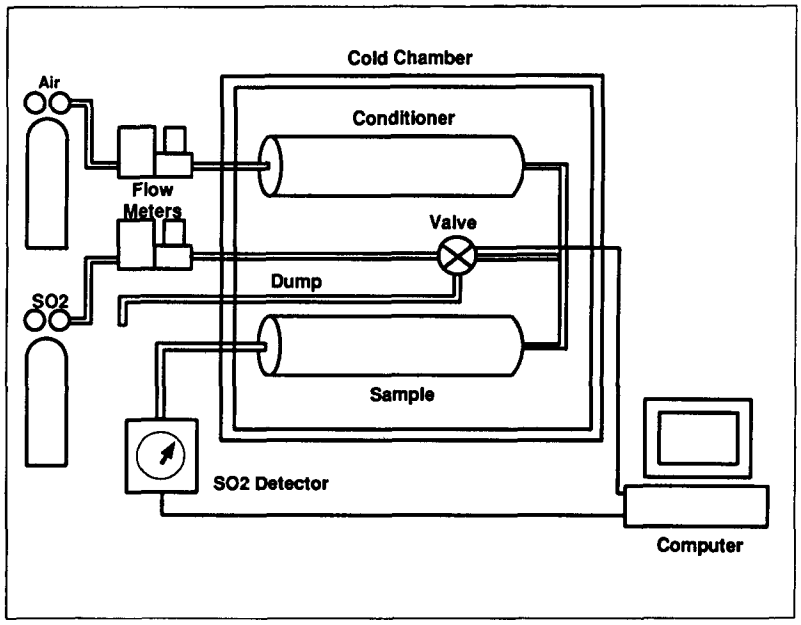

Fig. 1. Experimental apparatus.

Quantitative data, however, were available for SO_4^{2-} concentration from chemical analyses of the columns. At the end of each experiment, the column was divided into three sections; the front and back sections of the column were melted and the SO_4^{2-} concentrations were measured using an ion chromatograph (Dionex). The mean concentration was used as representative for the whole column. There was some evidence of channeling, as sometimes the back section had higher concentrations than the front section or vice versa. The remaining ice was used to make surface area measurements using stereological section plane analysis. The section preparation and analysis techniques used have been described by Perla (1982), Perla and Dozier (1984) and Perla *et al.* (1986).

To determine physical properties of the snow columns (i.e. dispersion), breakthrough curves were obtained for some of the ice columns using NO gas. Our previous results indicate that NO behaves similar to a conservative tracer (Sommerfeld *et al.*, 1992).

RESULTS

Both breakthrough curves for SO_2 and oxidation-product (SO_4^{2-}) concentration are used to interpret temperature and snow composition effects. Temperature dependence of sorption of SO_2 on ice is shown in Fig. 2. Shown are concentration vs time sorption curves for three ice compositions at four temperatures (-1, -8, -30 and -60°C). All three compositions show the same temperature pattern with minimum sorption at -30°C (typically, $-1 > -8 > -30 < -60$°C). The shape of the sorption curves changes with temperature. Two key features of the sorption curves are: (1) number of pore volumes before measurable amounts of SO_2 leaves the column and (2) the time it takes to approach equilibrium ($C/C_o = 1$). Curves at the warmer temperatures (-1 and -8°C) show a slow approach to equilibrium, as indicated by pronounced tailing. At the colder temperatures (-30 and -60°C) there is a delayed onset of the sorption curve, then a much faster approach to equilibrium, with the curves having close to a classic sigmoidal shape. In addition to the temperature dependence, comparing the three sets of curves illustrates the effects of changing the ice composition. In Fig. 2a, curves for all four temperatures reached equilibrium by 800 pore volumes. Addition of 10 μM NaCl delayed equilibrium attainment to over 1000 pore volumes for -1°C (Fig. 2b). Presence of an oxidant delayed equilibrium for all temperatures, with equilibrium not being reached for -1 and -8°C within 1500 pore volumes (Fig. 2c).

Figure 3 illustrates experimental reproducibility at three temperatures with and without H_2O_2. The sorption curves at -1, -8 and -30°C were highly reproducible. There were, however, some problems in reproducibility at -60°C. At that temperature, the O-rings that seal the column became brittle, and small leaks were more frequently observed. The effect of leaks was to displace the location of the sorption curves, not to change the shape of the curve.

These curves indicate that the largest change in the shape of the sorption curve occurs between -30 and -8°C, from a more sigmoidal shape to a non-symmetrical shape for higher temperatures. The effect of adding H_2O_2 can be seen as the difference between the two sets of curves for -1 and -8°C (Figs 3a and 3c). Without H_2O_2, there was a slower approach to equilibrium than would be expected from physical adsorption to a solid surface at the warmer temperatures. This could be due to slow uptake and diffusion into

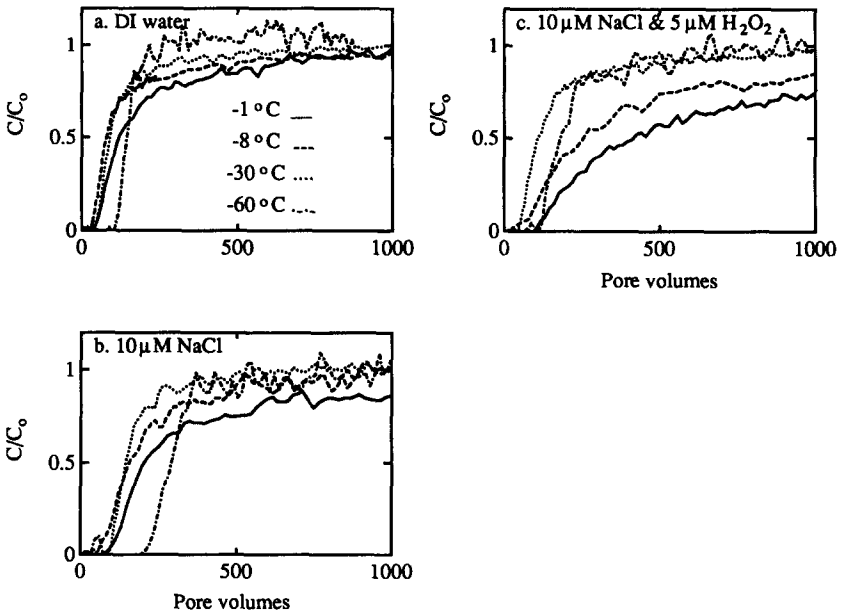

Fig. 2. Sorption limbs of SO_2 breakthrough curves at four temperatures on ice mixtures containing (a) deionized water, (b) 10 μM NaCl and (c) 10 μM NaCl and 5 μM H_2O_2.

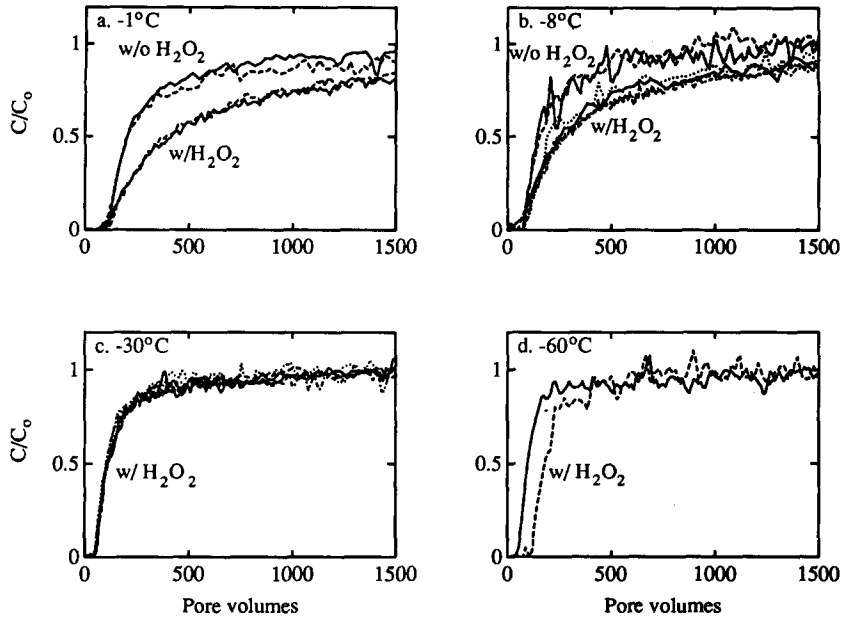

Fig. 3. Sorption limbs of SO_2 breakthrough curves showing reproducibility both with and without H_2O_2 on ice containing (a) 10 μM NaCl at -1°C, (b) 10 μM NaCl at -8°C, (c) 10 μM NaCl and 5 μM H_2O_2 at -30°C and (d) 10 μM NaCl and 5 μM H_2O_2 at -60°C.

the aqueous phase. There were trace levels of Fe present in the NaCl, so this slow uptake could also be due to Fe-catalysed oxidation of SO_2. The presence of H_2O_2 increases the time needed to approach equilibrium even further; slow uptake is thought to be due to oxidation and eventual depletion of H_2O_2 at the surface. At colder temperatures (e.g. -30°C, not shown), the presence of H_2O_2 does not change the shape of the curves, suggesting that there is a change in sorption mechanism between -30 and -8°C.

The shape of the sorption curves was not affected by dispersion in the columns. Sorption curves for NO on some of the same ice columns used for SO_2 are shown in Fig. 4. Compared to SO_2 curves, the NO curves exhibit a very sharp front; i.e. the rise in C/C_o from 0 to 1 occurs within 10 pore volumes. Typical retention volumes for the NO experiments were 7.5 to 8.5 pore volumes, showing increasing retention with decreasing temperature consistent with Sommerfeld *et al.* (1992).

To determine system losses (wall losses, etc.) an empty column of 5-cm length was used in place of the sample column. The measured retention volume was 45 pore volumes for -8°C. This represents an upper limit for system losses, since the introduction of an empty column changed the gas flow pattern in the column significantly. Previous experiments with NO in empty tubes indicated that experimental artifacts associated with the change in flow regime gave artificially high retention volumes (Sommerfeld, unpublished data). This retention volume was small relative to the total retention volume at -8°C for columns with ice spheres containing salt and oxidant.

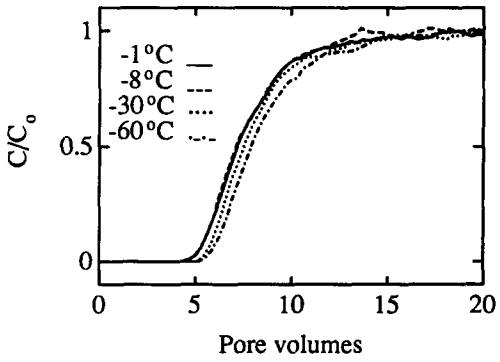

Fig. 4. Sorption limbs of NO breakthrough curves at four temperatures on ice containing 5 μM H_2O_2.

Representative full sorption and desorption curves are shown in Fig. 5 for two temperatures for ice containing 1 mM NaCl and 5 μM H_2O_2. The sorption and desorption curves show opposite trends with temperature. The sorption curve shows more tailing at the warmer temperature; there was more tailing in the desorption curve at -60°C. At -60°C, the sorption is more reversible in the presence of H_2O_2, indicating much less oxidation of SO_2. There is very little desorption at -1°C, indicating that most of the SO_2 is sorbed irreversibly, i.e. it is oxidized.

Analyses of the amount of SO_4^{2-} formed gave a lower limit for SO_2 uptake. The amount of SO_2 taken up by the ice, determined by melting the ice and measuring SO_4^{2-} concentrations, showed the same trends with respect to temperature and ice composition as did the sorption curves except for -60 and

Table 1. Production of SO_4^{2-} as a function of ice composition

Ice composition	Temp. (°C)	SO_4^{2-} formed ($g\,m^{-2} \times 10^{-7}$)*	H_2O_2 consumed (%)	No. of runs
Deionized H_2O	−60	2.0		1
10 μM NaCl	−60	7.9		1
1 mM NaCl	−60	17.7		1
5 μM H_2O_2	−60	15.8 ± 8.1	9	3
5 μM H_2O_2 and 10 μM NaCl	−60	25.5	14	1
5 μM H_2O_2 and 1 mM NaCl	−60	22.6	22	1
Deionized H_2O	−30	6.3 ± 1.1		4
10 μM NaCl	−30	3.7		2
1 mM NaCl	−30	24.8		2
5 μM H_2O_2	−30	26.4 ± 1.8	15	4
5 μM H_2O_2 and 1 mM NaCl	−30	45.6 ± 20.9	31	3
Deionized H_2O	−8	11.6 ± 1.1		5
10 μM NaCl	−8	14.3 ± 8.6		3
1 mM NaCl	−8	55.0 ± 11.2		3
5 μM H_2O_2	−8	84.7 ± 13.2	59	5
5 μM H_2O_2 and 10 μM NaCl	−8	82.3 ± 35.3	53	3
5 μM H_2O_2 and 1 mM NaCl	−8	111.4 ± 11.3	81	3
Deionized H_2O	−1	18.6 ± 2.0		5
10 μM NaCl	−1	26.3 ± 11.1		4
1 mM NaCl	−1	53.5 ± 17.2		4
5 μM H_2O_2	−1	109.4 ± 6.5	68	5
5 μM H_2O_2 and 10 μM NaCl	−1	86.1	71	2
5 μM H_2O_2 and 1 mM NaCl	−1	133.3 ± 21.4	92	3

* ± Represents 95% confidence intervals.

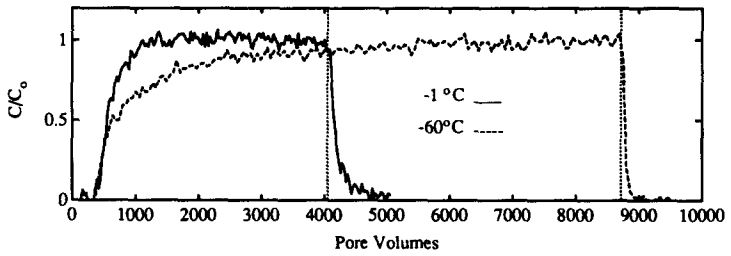

Fig. 5. Sorption and desorption limbs of SO_2 breakthrough curves for ice containing 5 μM H_2O_2 and 1 mM NaCl at −1 and −60°C. The vertical dotted lines indicate when desorption started.

−30°C (Table 1, Fig. 6). Most points represent the average of several experiments (the number of experiments are given in Table 1). At −60 and −30°C, SO_4^{2-} values significantly underrepresent the amount of SO_2 sorbed, as significant amounts of SO_2 desorbed at these temperatures (Fig. 4). The gas-phase concentration (69 vs 89 ppbv) did not affect the amount of SO_4^{2-} formed.

In the case where there was low NaCl (10 μM) and deionized water, the data are noisy, but the average concentration between the two ice compositions indicates that there was constant SO_4^{2-} formation at −60 and −30°C. A sharp increase in formation at −1 and −8°C, however, was observed. For the higher concentration of NaCl (1 mM), the trend with temperature was the same with and without H_2O_2, although there was a larger amount of SO_4^{2-} formed when H_2O_2 was present. At −60 and −30°C with 1 mM NaCl, the amount of SO_4^{2-} formed was significantly higher than the other ice compositions, with an exponential increase in SO_4^{2-} concentration between −60 and −8°C. Between −8 and −1°C, however, SO_4^{2-} concentration was not a function of temperature. In the ice with H_2O_2 only, there was an exponential increase with temperature over the whole range. These results indicate that oxidation occurred at all temperatures. At temperatures of −30°C and above, increasing the ionic strength had little effect on SO_4^{2-} for formation if H_2O_2 is present, but strongly influenced SO_2 uptake in its absence. This may be due to two effects: (1)

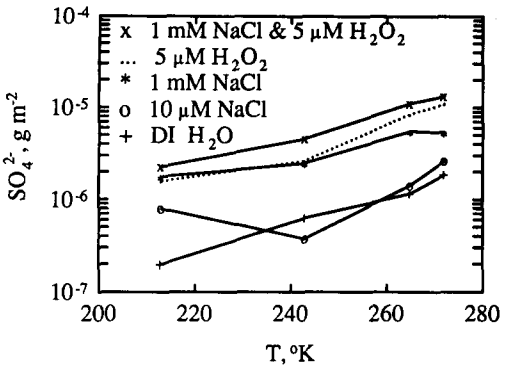

Fig. 6. Average mass SO_4^{2-} produced per ice surface area at different temperatures for different ice mixtures. Ninety five per cent confidence intervals are given in Table 1.

increase in the depth of the disordered layer and (2) oxidation catalysed by trace amounts of Fe(III) in the NaCl.

There was little SO_2 degassing at the warmer temperatures (−1 and −8°C). Thus, the chemical analyses of SO_4^{2-} should reflect the total amount of SO_2 taken up. At lower temperatures, however, it underpredicts the total amount. However, there is an inconsistency between the sorption curve results in estimating SO_2 uptake and those from the chemical analyses of SO_4^{2-}. The sorption curve results all gave lower total sorption values than the chemical analyses; this is attributed to the uncertainty in determining C_o.

The stoichiometry of the SO_2 oxidation reaction allows the calculation of the upper limit of H_2O_2 depleted (i.e. assuming a 1:1 stoichiometry). These results are shown in Table 1. The calculation shows that up to 90% of the H_2O_2 was consumed at −1°C with 1 mM NaCl. At −60°C, with no NaCl present, only 5% or less of the H_2O_2 was consumed.

DISCUSSION

For aqueous-phase reactions to occur on ice surfaces, the surface must have liquid-like properties or liquid water must be present. Near the melting temperature of ice, a disordered layer is formed. This has been called the surface pre-melt layer or quasi-liquid layer. Considerable evidence supports the presence of this layer at temperatures as low as −10°C, but its thickness and bulk properties are not well defined (e.g. Kvilividze *et al.*, 1974; Golecki and Jaccard, 1978; Beaglehole and Nason, 1980; Ocampo and Klinger, 1983; Nenow, 1984). Furthermore, the effect of high levels of impurities on the surface of the ice crystal on this layer are not known, but high concentrations of impurities may disrupt the crystal structure.

Temperature, ionic strength and presence of oxidant all affected SO_2 uptake on ice spheres. A general trend can be observed in the breakthrough curves and SO_4^{2-} data; the sorption of SO_2 increased with rising temperature for all ice compositions above −30°C. At −60°C, breakthrough curves indicated an increase in SO_2 sorption; the SO_4^{2-} concentration did not echo this trend, but it represents a lower limit due to desorption. The effect of oxidant and salt concentration can be seen as higher SO_2 uptake for 1 mM NaCl and 5 μM H_2O_2, both with and without NaCl present at all temperatures greater than −30°C. At −30, −8 and −1°C, the uptake was up to three-fold greater with H_2O_2 than without for 1 mM NaCl. An increasing thickness of the surface pre-melt layer with increasing ionic strength is consistent with freezing-point depression and increased SO_2 uptake.

Liquid water can be present in snow at temperatures below 0°C due to freezing-point depression from the presence of solutes. Surface curvature may result also in an equilibrium temperature between ice and liquid water that is lower than 0°C (Colbeck, 1980). Due to curvature, essentially all of the liquid water in stable grain clusters (at temperatures both at and below 0°C) should be in the veins or fillets (Colbeck, 1979). Furthermore, concentrations of solutes might be expected to be high in the areas where water resides. Mulvaney *et al.* (1988) have shown evidence that solutes are concentrated in triple junction points of ice particles.

The shape of the breakthrough-curve sorption curves varied with temperature, from a nearly sigmoidal shape at −60°C to a gradually more non-symmetrical shape as the temperature increased. Non-symmetrical shapes have been attributed to rate-limiting chemical or physical processes (e.g. van Genuchten and Wierenga, 1976; van Genuchten and Dalton, 1986). Based on our NO data where only reversible adsorption is observed, simple physical adsorption for the SO_2 system can be ruled out. At −1°C, the desorption curve showed an abrupt decrease in concentration once the SO_2 was turned off. When H_2O_2 is present, S(IV) should be oxidized to S(VI) on the surface and thus cannot be desorbed. At −60°C the sorption curve was more symmetrical and the sorption and desorption curves had similar shapes. The desorption curve showed more tailing than at the higher temperatures, showing more desorption of the SO_2. This is because much less of the sorbed SO_2 was oxidized to SO_4^{2-} and can thus be desorbed.

The results from both the breakthrough curve shapes and the production of SO_4^{2-} indicate an effect of surface pre-melting on the chemical properties of the ice surface down to −30°C. This supports the observations of Sommerfeld and Lamb (1986) on SO_2 sorption on ice as a function of temperature. In contrast, other theoretical and experimental work suggest that the surface disorder is not important below about −10°C (Hobbs, 1974). The difference may be the result of the different methods used to detect the surface characteristics. It may also be the result of an influence of the composition of the ice used. The addition of solutes to the surface pre-

melt layer would increase its equilibrium thickness and thus lower the temperature at which it is detectable.

In the case of H_2O_2, an additional liquid phase may also be present on the grain surfaces. Giguère and Geoffrion (1950) show a phase diagram in which a liquid solution of an H_2O–H_2O_2 addition compound (suggested to be $H_2O_2 \cdot 2H_2O$) in water is stable down to a eutectic point at $-53°C$. They suggest that separate solid phases exist for H_2O and H_2O_2–H_2O addition compound form below the eutectic point. Upon melting H_2O/H_2O_2 mixtures, H_2O_2 gas is evolved, perhaps because the H_2O_2 is so distorted in the crystal structure. This suggests that the H_2O_2 is excluded from the bulk ice during metamorphism and is relocated on the grain boundaries. Results of SO_4^{2-} formation at $-1°C$ indicate most of the H_2O_2 was consumed during the experiment (Table 1). This would be possible only if the majority of the H_2O_2 is found on, or could readily move to, the reacting surfaces of the ice particles (i.e. at grain boundaries).

The chemical composition of the ice surface depends on the partitioning of chemical species between the ice crystal structure and the surface during crystal growth or metamorphism. During rapid formation of ice, impurities should be distributed throughout the grain; slower growth or metamorphism should result in concentration near the surface. This is because the presence of an impurity would cause a greater lattice strain in the crystal than it would at a grain boundary (which is more disordered). Preliminary results suggest even freezing in liquid N_2 results in grain-scale concentration gradients (Petersen, 1990). Oxidants may also be concentrated on the ice surface. For example, the partitioning ratio of H_2O_2 between ice and water is 0.01 (Sigg *et al.*, 1987).

The partition ratio of NaCl between ice and water is in the range 10^{-3}–10^{-4} (Gross, 1968; Gross *et al.*, 1975). Thus, NaCl will also be excluded from the ice lattice during the freezing and metamorphic processes. Results by Bales (1992) suggest that freezing 200-μm droplets in liquid N_2 is "slow" and results in polycrystalline spheres with only small grain-scale concentration gradients. The experimental results demonstrate that oxidation reactions can occur down to temperatures of $-60°C$ in the presence of NaCl, suggesting that there should be a significant fraction of the total NaCl on the reacting surfaces.

There were some severe problems associated with detector drift that degraded the accuracy of quantitative analyses from the breakthrough curves. The inconsistency of the total adsorption determined from the breakthrough curves compared to the amount converted to SO_4^{2-} is not adequately explained. It is most likely the result of the drift problems in the SO_2 detector that make the estimation of the equilibrium attainment time difficult. However, the existence of this inconsistency leaves a question concerning the accuracy of the data. The good qualitative agreement provides good evidence for the basic conclusion concerning the different adsorption mechanisms, depending on the physical and chemical conditions. We believe the conclusions to be valid although the numbers may be subject to some uncertainty.

CONCLUSIONS

Our results show that at temperatures at above $-8°C$, the ice surface can be modeled as an aqueous phase, even at low ionic strengths resulting from SO_2 uptake onto ice made from deionized H_2O. At and below $-30°C$, physical adsorption apparently dominates. Oxidation of SO_2 by H_2O_2 can occur at all temperatures studied. However, availability of oxidant near the surface is greater at higher temperatures. At $-1°C$ most of the oxidant is apparently accessible for reactions in the surface layer.

To put these results in the context of dry deposition onto snow, the phenomenon that we are studying is the role of surface resistance in controlling rates of dry deposition of reactive gases to snow. The results show that snow exposed to background levels of SO_2 can accumulate acidity and ionic species on the particle surfaces. The location of the ionic species and acids on ice particles would facilitate the development of an ionic pulse during the early stages of snowmelt, which has been observed in the Sierra Nevada (Williams and Melack, 1991) and other locations. The concentrations used in this study were higher than found in most natural settings. In general, higher SO_2 concentrations should lead to higher deposition velocities (Bales *et al.*, 1987), however, the total SO_2 deposited will be highly dependent on the amount of available oxidant and the characteristics of the pre-melt layer. Our results also show that a simple constant surface resistance is not sufficient to model the deposition of SO_2 to snow. The composition of the snow, the temperature, and the flux from the atmosphere compared to the reaction rate on the ice surface may affect the value of the surface resistance. These parameters must be taken into account in dry deposition modeling.

Acknowledgements—This research was supported by the National Science Foundation, under grant ATM-8909460, and U.S. Forest Service, Rocky Mountain Experiment Station, under project 28-CO-522. Discussions with Roger Bales were very helpful in conducting this work.

REFERENCES

Bales R. C. (1992) Snowmelt and the ionic pulse. In *The Encyclopedia of Earth Science*, Vol. 1, pp. 199–207. Academic Press, Orlando, FL.

Bales R. C., Valdez M. P. and Dawson G. A. (1987) Gaseous deposition to snow: II. Physical–chemical model for SO_2 deposition, *J. geophys. Res.* **92,** 9789–9799.

Beaglehole D. and Nason D. (1980) Transition layer on the surface on ice. *Surf. Sci.* **96,** 357–363.

Clapsaddle C. and Lamb D. (1989) The sorption behavior of SO_2 on ice at temperatures between $-30°C$ and $-5°C$. *Geophys. Res. Lett.* **16,** 1173–1176.

Colbeck S. C. (1979) Grain clusters in wet snow. *J. Colloid Interf. Sci.* **72,** 371–384.

Colbeck S. C. (1980) Thermodynamics of snow metamorphism due to variations in curvature. *J. Glaciol.* **26,** 291–301.

Crittenden J. C., Hutzler N. J., Geyer D. G., Oravitz J. L. and Friedman G. (1986) Transport of organic compounds with saturated groundwater flow: model development and parameter sensitivity. *Wat. Resour. Res.* **22,** 271–284.

Giguère P. A. and Geoffrion P. (1950) Changes of density of hydrogen peroxide solutions on cooling and freezing. *Can. J. Res. B.* **28,** 599–607.

Golecki I. and Jaccard C. (1978) Intrinsic surface disorder in ice near the melting point. *J. Phys. C: Solid State Phys.* **11,** 4229–4237.

Gross G. W. (1968) Some effects of trace inorganics on the ice/water system. In *Trace Inorganics in Water*, Adv. Chem. Ser. Vol. 73, pp. 27–97. American Chemical Society, Washington, DC.

Gross G. W., Wu C., Bryant L. and McKee C. (1975) Concentration dependent solute redistribution at the ice/water phase boundary. II. Experimental investigation. *J. chem. Phys.*, **62,** 3085–3092.

Gunz D. W. and Hoffmann M. R. (1990) Field investigation on the snow chemistry in Central and Southern California—I. Inorganic ions and hydrogen peroxide. *Atmospheric Environment* **24A,** 1661–1671.

Hobbs P. (1970) *Ice Physics.* Clarendon Press, Oxford.

Hoffmann M. R. and Calvert J. G. (1985) *Chemical Transformation Modules for Eulerian Acid Deposition Models*, Vol. II, The Aqueous Chemistry, 1985. U.S. EPA, NCAR interagency agreement DW 930237.

Iribarne J. V. and Pyshnov T. (1990) The effect of freezing on the composition of supercooled droplets — I. Retention of HCl, HNO_3, NH_3 and H_2O_2. *Atmospheric Environment* **24A,** 383–387.

Kvlividze V. I., Kiselev V. F., Kurzaev A. B. and Ushakova L. A. (1974) The mobile water phase on ice surfaces. *Surf. Sci.* **44,** 60–68.

Mulvaney R., Wolff E. W. and Oates K. (1988) Sulphuric acid at grain boundaries in ice. *Nature* **331,** 247–249.

Neftel A., Jacob P. and Klockow D. (1984) Measurements of hydrogen peroxide in polar ice samples. *Nature* **311,** 43–45.

Nenow D. (1984) Surface premelting. *Prog. Crystal Growth Char* **9,** 185–225.

Ocampo J. and Klinger J. (1983) Modification of the surface structure of ice during aging *J. phys. Chem.* **87,** 4167–4170.

Perla R. (1978) Snow crystals, Paper 1. National Hydrology Research Institute, Environment Canada, Ottawa.

Perla R. and Dozier J. (1984) Observations on snow structure. In *Proc. 6th Int. Snow Science Workshop*, pp. 182–187, Mountain-Rescue, Aspen, CO.

Perla R., Dozier J. and Davis R. E. (1986) Preparation of Serial sections in dry snow specimens. *J. Microsc.* **142,** 111–114.

Petersen C. E. (1990) Ion Flux through a shallow snowpack: effects of initial and melt conditions. M. S. thesis, Department of Hydrology and Water Resources, The University of Arizona, Tucson.

Roberts P. V., Goltz M., Summers R., Crittenden J. C. and Nkedi-Kizza P. (1987) The influence of mass transfer on solute transport in column experiments with an aggregate soil. *J. Contam. Hydrol.* **1,** 375–393.

Sigg A., Neftel A. and Zurcher F. (1987) Chemical transformations in a snow cover at Weissfluchjoch, Switzerland, situated at 2500 m.a.s.l. In *Seasonal Snowcovers: Physics, Chemistry, Hydrology* (edited by Jones H. G. and Orville-Thomas W. J.). NATO Advanced Studies Institute. Reidel, Amsterdam.

Sommerfeld R. A. and Freeman T. L. (1988) Making artificial snow for laboratory use. USDA Forest Service research note RM-486.

Sommerfeld R. A. and Lamb D. (1986) Preliminary measurements of SO_2 adsorbed on ice. *Geophys Res. Lett.* **13,** 349–351.

Sommerfeld R. A., Conklin M. H. and Laird K. (1992) NO adsorption on ice at low concentrations. *J. Colloid Interf. Sci.* **149,** 569–574.

Valdez M. P., Bales R. C., Stanley D. A. and Dawson G. A. (1987) Gaseous deposition to snow: I. Experimental study of SO_2 and NO_2 deposition. *J. geophys. Res.* **92,** 9779–9789.

Van Genuchten M. Th. and Dalton F. N. (1986) Models for simulating salt movement in aggregated field soils. *Geoderma* **38,** 165–183.

Van Genuchten M. Th. and Wierenga P. J. (1976) Numerical solution for convective dispersion with intra-aggregate diffusion and non-linear adsorption. In *System Simulation in Water Resources* (edited by Vansteenkiste C. G.), pp. 275–291. North-Holland, Amsterdam.

Williams M. W. and Melack J. M. (1991) Solute chemistry of snowmelt and runoff in an alpine basin, Sierra Nevada. *Wat. Resour. Res.* **27,** 1575–1588.